BIOCHEMISTRY
including biophysical chemistry & molecular biology
*Article*

*Biochemistry* **2009,** *48,* 12305–12313 12305
DOI: 10.1021/bi901694s

# Mechanistic Studies of *para*-Substituted *N*,*N*′-Dibenzyl-1,4-diaminobutanes as Substrates for a Mammalian Polyamine Oxidase[†]

Michelle Henderson Pozzi,[‡] Vijay Gawandi,[‡] and Paul F. Fitzpatrick*,[§]

[‡]*Department of Biochemistry and Biophysics, Texas A&M University, College Station, Texas 77843-2128 and* [§]*Department of Biochemistry, University of Texas Health Science Center at San Antonio, San Antonio, Texas 78229-3900*

*Received September 29, 2009; Revised Manuscript Received November 12, 2009*

ABSTRACT: The kinetics of oxidation of a series of *para*-substituted *N*,*N*′-dibenzyl-1,4-diaminobutanes by the flavoprotein polyamine oxidase from mouse have been determined to gain insight into the mechanism of amine oxidation by this member of the monoamine oxidase structural family. The $k_{cat}/K_m$ values are maximal at pH 9, consistent with the singly charged substrate being the active form. The rate constant for flavin reduction, $k_{red}$, by *N*,*N*′-dibenzyl-1,4-diaminobutane decreases about 5-fold below a p$K_a$ of ~8; this is attributed to the need for a neutral nitrogen at the site of oxidation. The $k_{red}$ and $k_{cat}$ values are comparable for each of the *N*,*N*′-dibenzyl-1,4-diaminobutanes, consistent with rate-limiting reduction. The deuterium kinetic isotope effects on $k_{red}$ and $k_{cat}$ are identical for each of the *N*,*N*′-dibenzyl-1,4-diaminobutanes, consistent with rate-limiting cleavage of the substrate CH bond. The $k_{red}$ values for seven different *para*-substituted *N*,*N*′-dibenzyl-1,4-diaminobutanes correlate with a combination of the van der Waals volume and $\sigma$ value of the substrates, with $\rho$ values of $-0.59$ at pH 8.6 and $-0.09$ at pH 6.6. These results are consistent with direct transfer of a hydride from the neutral CN bond of the substrate to the flavin as the mechanism of polyamine oxidase.

The polyamines spermine and spermidine are critical for growth of eukaryotic cells due to the ability of these polycations to bind a variety of macromolecules (*1*). As a result polyamine metabolism has been a frequent target for the development of anticancer agents (*2*). Catabolism of spermine and spermidine can occur by two routes (*3*). In the first pathway to be discovered, spermidine/spermine *N*1-acetyltransferase converts spermine or spermidine to the *N*-acetyl form (*4*). The *N*1-acetylspermine or *N*1-acetylspermidine can then be transported out of the cell. Alternatively, the flavoprotein polyamine oxidase (PAO)[1] can catalyze the oxidation of *N*1-acetylspermine and *N*1-acetylspermidine to spermidine and putrescine, respectively, producing $H_2O_2$ (*5*, *6*). The more recently discovered flavoprotein spermine oxidase catalyzes the oxidation of spermine directly to spermidine (*7*, *8*), bypassing the necessity for acetylation. While PAO is a constitutive enzyme, spermine oxidase is induced by polyamine analogues with antitumor activity (*7*). The relative importance of the two enzymes in polyamine metabolism in normal and cancer cells remains to be established.

PAO belongs to the flavin amine oxidase structural family that includes monoamine oxidase A and B (MAO A/B) (*9*), lysine-specific demethylase (LSD1) (*10*), and L-amino acid oxidase (*11*). At present there is no structure available of a mammalian PAO, and the sequence identity of mouse or human PAO to these enzymes is low (< 20%). Still, structures are available of maize PAO and yeast Fms1 that establish that these two enzymes and mammalian PAOs belong to the MAO structural family (*12*). However, PAO from maize and other plants catalyzes CH bond cleavage on the *endo*-side of the N4-nitrogen of spermine and *N*1-acetylspermine (*13*), whereas mammalian PAOs catalyze CH bond cleavage on the *exo*-side of the N4-nitrogen, and Fms1 is more accurately a spermine oxidase than a PAO, in that its preferred substrate is spermine rather than *N*1-acetylspermine (*14*). The structural basis for the differences in reactivity remains unknown.

The reaction of PAO, like other flavoprotein amine oxidases, can be divided into two half-reactions. In the reductive half-reaction a hydride equivalent is transferred from the amine substrate to the flavin to form the reduced flavin and the oxidized amine; in the oxidative half-reaction the reduced flavin reacts with molecular oxygen to produce hydrogen peroxide and the oxidized flavin. Mouse PAO displays the ping-pong kinetic pattern (*5*) observed with most flavoprotein oxidases (*15*), since oxygen only reacts with the reduced enzyme formed upon oxidation of the amine. The mechanism by which electrons are transferred from the amine substrate to the flavin by the flavin amine oxidases has been controversial (*16*). The simplest mechanism is direct hydride transfer; this is supported by the lack of detectable intermediates in the reductive half-reactions of flavin amine oxidases and by kinetic isotope effects (*17*−*21*). The ability of compounds containing cyclopropyl rings to act as mechanism-based inhibitors of MAO has been taken as evidence for radical intermediates in the reactions of that enzyme and other flavin amine oxidases (*22*). Finally, a mechanism involving nucleophilic addition of the amine substrate to the flavin has been proposed (*23*). In the present study, *para*-substituted *N*,*N*′-dibenzyl-1,4-diaminobutanes were characterized as substrates for mouse PAO to gain insight into the substrate specificity and mechanism of amine oxidation by that enzyme.

---

[†]This work was supported in part by grants from the NIH (R01 GM58698) and The Welch Foundation (AQ-1245).

*Address correspondence to this author. Phone: 210-567-8264. Fax: 210-567-8778. E-mail: fitzpatrick@biochem.uthscsa.edu.

[1]Abbreviations: PAO, polyamine oxidase; MAO, monoamine oxidase; LSD1, lysine-specific demethylase.

## EXPERIMENTAL PROCEDURES

*Materials.* Reagents for syntheses were routinely purchased from Aldrich Chemical Co. *N*1-Acetylspermine was from Fluka. All remaining reagents were of the highest purity commercially available.

*Syntheses. Deuterated Benzaldehydes.* Commercially available 4-substituted benzoic acids were converted to the corresponding benzyl-deuterated benzaldehydes by modification of the method of Paik et al. (*24*). Lithium aluminum deuteride (1.2 g, 28.5 mmol) was added in small portions to a stirred solution of the *para*-substituted benzoic acid (7.4 mmol) in anhydrous THF (20 mL) at −20 °C over 4 h. The solution was then warmed to room temperature for 1 h. The reaction was quenched with saturated aqueous $NH_4Cl$ (30 mL). Twenty milliliters of 10% NaOH was added; after 1 h 15 mL of water was added. The resulting precipitate was filtered off and washed with ether. The combined organic layers were evaporated under vacuum. The remaining oil was dried under vacuum and dissolved in anhydrous $CH_2Cl_2$ (40 mL) at 4 °C. Pyridinium chlorochromate (5.0 g, 23 mmol) was added, and the reaction mixture was stirred for 40 min in an ice bath and then quenched with 75 mL of saturated aqueous $NaHCO_3$. The combined organic layers from three extractions with ethyl acetate (50 mL each) were washed with water and brine and then dried over anhydrous $Na_2SO_4$. Column chromatography on silica gel with 5% ethyl acetate in hexane yielded the deuterated benzaldehyde as a colorless oil.

*N,N′-Dibenzyl-1,4-butanediamines.* The synthesis was adapted from Burns et al. (*25*). The appropriate benzaldehyde (12.5 mmol) and triethylamine (1.74 mL, 12.5 mmol) were added to a solution of 1,4-diaminobutane (0.5 g, 5.7 mmol) in 20 mL of dichloromethane, followed by 0.5 g of $MgSO_4$. The reaction mixture was stirred overnight at room temperature and then filtered. The solvent was removed under reduced pressure. The residue was dissolved in 20 mL of methanol, and $NaBH_4$ (0.56 g, 13.4 mmol) was added. After being stirred overnight at room temperature, 25 mL of water was added, followed by sufficient 2 M NaOH to yield pH 10−11. The solution was extracted three times with 25 mL of dichloromethane. The combined organic phases were dried over $MgSO_4$ and filtered. The volume was decreased to ∼5 mL under reduced pressure. Concentrated HCl was added dropwise until a white precipitate appeared. The precipitate was collected by filtration, washed with dry diethyl ether, and recrystallized from water/2-propanol. For the deuterated compounds, the respective deuterated benzaldehyde and $NaBD_4$ were used.

*N,N′-Dibenzyl-1,4-butanediamine dihydrochloride*: yield 1.5 g (75%); mp 327 °C; $^1$H NMR ($D_2O$) $\delta$ 7.38 (10H), 4.66 (4H, s), 2.98 (4H, m), 1.64 (4H, m). HRMS (m+H): theor, 269.19; found, 269.21.

*N,N′-Bis(p-N,N-dimethylaminobenzyl)-1,4-butanediamine tetrahydrochloride*: yield 1.1 g (78%); mp 244 °C; $^1$H NMR ($D_2O$) $\delta$ 7.72 (4H, d), 7.68 (4H, d), 4.33 (4H, s), 3.31 (12H, s), 3.16 (4H, t), 1.81 (4H, m). HRMS (m + H): theor, 355.28; found, 355.21.

*N,N′-Bis(p-methoxybenzyl)-1,4-butanediamine dihydrochloride*: yield 1.03 g (61%); mp 301 °C; $^1$H NMR ($D_2O$) $\delta$ 7.32 (4H, d), 6.93 (4H, d), 3.84 (6H, s), 3.81 (4H, s), 2.65 (4H, t), 1.57 (4H, m, $CH_2$). HRMS (m + H): theor, 329.22; found, 329.25.

*N,N′-Bis(p-methylbenzyl)-1,4-butanediamine dihydrochloride*: yield 1.4 g (67%); mp 331 °C; $^1$H NMR ($D_2O$) $\delta$ 7.24 (4H, d), 7.18 (4H, d), 4.23 (4H, s), 2.42 (6H, s), 3.06 (4H, t), 1.92 (4H, m). HRMS (m + H): theor, 297.23; found, 297.21.

*N,N′-Bis(p-chlorobenzyl)-1,4-butanediamine dihydrochloride*: yield 1.31 g (62%); mp 334 °C; $^1$H NMR ($D_2O$) $\delta$ 7.42 (4H, d), 7.33 (4H, d), 4.11 (4H, s), 2.99 (4H, t), 1.67 (4H, m). HRMS (m + H): theor, 337.12; found, 337.1.

*N,N′-Bis(p-bromobenzyl)-1,4-butanediamine dihydrochloride*: yield 1.31 g (62%); mp 333 °C; $^1$H NMR ($D_2O$) $\delta$ 7.45 (4H, d), 7.36 (4H, d), 4.15(4H, s), 3.09 (4H, t), 1.85 (4H, m). HRMS (m + H): theor, 425.01; found, 425.04.

*N,N′-Bis(p-trifluoromethylbenzyl)-1,4-butanediamine dihydrochloride*: yield 1.35 g (66%); mp 327 °C; $^1$H NMR ($D_2O$) $\delta$ 7.57 (4H, d), 7.45 (4H, d), 3.84 (4H, s), 2.64 (4H, t), 1.57 (4H, m). HRMS (m + H): theor, 405.17; found, 405.12.

*N,N′-Bis(p-N,N-dimethylamino-α,α-dideuteriobenzyl)-1,4-butanediamine tetrahydrochloride*: yield 0.85 g (89%); $^1$H NMR ($D_2O$) $\delta$ 7.74 (4H, d), 7.69 (4H, d), 3.35 (12H, s), 3.19 (4H, t), 1.83 (4H, m). HRMS (m + H): theor, 359.28; found, 359.01.

*N,N′-Bis(p-methoxy-α,α-dideuteriobenzyl)-1,4-butanediamine dihydrochloride*: yield 0.93 g (87%); $^1$H NMR ($D_2O$) $\delta$ 7.33 (4H, d), 6.98 (4H, d), 3.87 (6H, s), 2.68 (4H, t), 1.60 (4H, m). HRMS (m + H): theor, 333.22; found, 333.04.

*N,N′-Bis(p-methyl-α,α-dideuteriobenzyl)-1,4-butanediamine dihydrochloride*: yield 0.85 g (87%); $^1$H NMR ($D_2O$) $\delta$ 7.22 (4H, d), 7.18 (4H, d), 2.45 (6H, s), 3.12 (4H, t), 1.95 (4H, m). HRMS (m + H): theor, 300.23; found, 301.05.

*N,N′-Bis(α,α-dideuteriobenzyl)-1,4-butanediamine dihydrochloride*: yield 0.63 g (85%); $^1$H NMR ($D_2O$) $\delta$ 7.41 (10H, m), 3.05 (4H, t), 1.65 (4H, m). HRMS (m + H): theor, 273.22; found, 273.11.

*N,N′-Bis(p-chloro-α,α-dideuteriobenzyl)-1,4-butanediamine dihydrochloride*: yield 0.74 g (84%); $^1$H NMR ($D_2O$) $\delta$ 7.44 (4H, d), 7.34 (4H, d), 3.01 (4H, t), 1.68 (4H, m). HRMS (m + H): theor, 341.12; found, 341.00.

*N,N′-Bis(p-bromo-α,α-dideuteriobenzyl)-1,4-butanediamine dihydrochloride*: yield 0.85 g (87%); $^1$H NMR ($D_2O$) $\delta$ 7.46 (4H, d), 7.37 (4H, d), 3.11 (4H, t), 1.86 (4H, m). HRMS (m + H): theor, 429.01; found, 429.91.

*N,N′-Bis(p-trifluoromethyl-α,α-dideuteriobenzyl)-1,4-butanediamine dihydrochloride*: yield 0.86 g (84%); $^1$H NMR ($D_2O$) $\delta$ 7.58 (4H, d), 7.47 (4H, d), 2.66 (4H, t), 1.58 (4H, m). HRMS (m + H): theor, 409.17; found, 409.04.

*N,N′-Dibenzyl-1,2-diaminoethane* was synthesized in a similar fashion from diaminoethane (0.5 g) and benzaldehyde (1.9 g): yield 1.3 g (65%); $^1$H NMR ($D_2O$) $\delta$ 7.39 (10H, m), 4.20 (4H, s), 3.37 (4H, t). HRMS (m + H): theor, 241.16; found, 241.27.

*N,N′-Dibenzyl-1,3-diaminopropane* was synthesized in a similar fashion from diaminopropane (1.0 g) and benzaldehyde (3.2 g): yield 2.5 g (66%); $^1$H NMR ($D_2O$) $\delta$ 7.39 (10H, m), 4.15 (4H, s), 3.05 (4H, t), 2.05 (2H, p). HRMS (m + H): theor, 255.18; found, 255.19.

*Expression and Purification of PAO.* His-tagged mouse PAO was purified from BL21(DE3) *Escherichia coli* cells as described previously (*26*). The concentration of active enzyme was determined using an $\varepsilon_{458}$ value of 10400 $M^{-1}$ $cm^{-1}$ (*20*).

*Steady-State Assays.* Steady-state kinetic parameters for PAO were determined using a computer-interfaced Clark oxygen electrode (Hansatech Instruments) to measure the initial rate of oxygen consumption. All assays were performed at 30 °C and were initiated by addition of enzyme to a final concentration of 0.1−0.5 $\mu$M. The buffers were 50 mM Tris-HCl for pH 7.1−8.6, 50 mM CHES for pH 9.1−9.6, and 50 mM CAPS at pH 10.1. All buffers contained 10% glycerol. The concentrations of substrates were determined enzymatically, measuring the amount of oxygen required to completely oxidize a limiting amount of the substrate; the concentration of each substrate based on this assay was consistently twice that based on molecular weight, indicating an ability of PAO to recognize and oxidize both sides of $N,N'$-dibenzyl-1,4-diaminobutanes.

*Rapid Reaction Kinetics.* Rapid reaction kinetic measurements were performed on an Applied Photophysics SX-18MV stopped-flow spectrophotometer using both single wavelength and photodiode array detection. To establish anaerobic conditions, the instrument was loaded with anaerobic buffer containing 5 mM glucose and 36 nM glucose oxidase and left overnight. Enzyme solutions (~40 $\mu$M) containing 5 mM glucose were made anaerobic by applying cycles of argon and vacuum; substrate solutions containing 5 mM glucose were made anaerobic by bubbling with argon. Glucose oxidase was added to all anaerobic solutions at a final concentration of 36 nM. For each substrate, the rate constant for reduction was determined as a function of amine concentration, and the results were fit to the Michaelis–Menten equation to obtain the $k_{red}$ value.

*Data Analysis.* Data were analyzed using the programs KaleidaGraph (Adelbeck Software, Reading, PA) and Igor (WaveMetrics, Lake Oswego, OR). Initial rate data were fit to the Michaelis–Menten equation to determine steady-state kinetic parameters. $k_{cat}/K_m$–pH profiles were fit to eq 1, where $y$ is the $k_{cat}/K_m$ value at a given pH, $c$ is its pH-independent value, $K_1$ is the ionization constant for a moiety that must be unprotonated for activity, and $K_2$ is the ionization constant for a moiety that must be protonated for activity (*27*). Kinetic isotope effects on steady-state parameters were determined from fits to eq 2 or 3 (*28*, *29*), where $E$ is the isotope effect on $k_{cat}/K_m$ and $k_{cat}$, $s$ is the concentration of substrate, and $F_i$ is the fraction of heavy isotope in the substrate. Some of the substrates exhibited substrate inhibition and were consequently fit with eq 3, where $K_{ai}$ is the substrate inhibition constant.

$$\log y = \log[c/(1+H/K_1+K_2/H)] \quad (1)$$

$$v = (k_{cat}s)/((K_m+s)(1+(E-1)F_i)) \quad (2)$$

$$v = (k_{cat}s)/(K_m(1+F_i(E-1))+s(1+F_i(E-1))+s^2/K_{a1}) \quad (3)$$

Rapid reaction kinetic traces were fit as single or double exponential decays (eqs 4 and 5); here, $k_1$ and $k_2$ are the first-order rate constants for the two phases, $A_1$ and $A_2$ are the absorbance changes associated with the two phases, $A_t$ is the total absorbance change, and $A_\infty$ is the final absorbance. The $k_{red}$–pH profile was fit to eq 6, where $y$ is the value of $k_{red}$ at a given pH, $y_L$ is its limiting value at low pH, $\Delta y$ is the difference in $k_{red}$ at high and low pH, and $K_1$ is the ionization constant for the transition (*27*).

$$A_t = A_1 e^{-k_1 t} + A_\infty \quad (4)$$

$$A_t = A_1 e^{-k_1 t} + A_2 e^{-k_2 t} + A_\infty \quad (5)$$

$$\log y = \log(y_L + (\Delta y/(1+H/K_1))) \quad (6)$$

## RESULTS

*$N,N'$-Dibenzyldiamines as Substrates.* Several $N,N'$-dibenzyldiamines were previously shown to be substrates for partially purified polyamine oxidase from pig liver, producing benzaldehyde as product; the highest activity was seen with the 1,3-diaminopropane and 1,4-diaminobutane derivatives (*30*). With the purified recombinant mouse enzyme in hand, we determined the kinetics of oxidation of $N,N'$-dibenzyl-1,2-diaminoethane, $N,N'$-dibenzyl-1,3-diaminopropane, and $N,N'$-dibenzyl-1,4-diaminobutane in air-saturated buffer at pH 8.6. No activity was detected with the diaminoethane derivative. The apparent $k_{cat}$, $K_m$, and $k_{cat}/K_m$ values for $N,N'$-dibenzyl-1,3-diaminopropane were 6.1 ± 0.2 $s^{-1}$, 40 ± 6 $\mu$M, and 0.15 ± 0.02 $\mu M^{-1}\ s^{-1}$, respectively. For $N,N'$-dibenzyl-1,4-diaminobutane, the values of these kinetic parameters were 0.80 ± 0.02 $s^{-1}$, 15 ± 2 $\mu$M, and 0.054 ± 0.004 $\mu M^{-1}\ s^{-1}$. The latter $K_m$ value is within a factor of 2 of the value reported for the pig enzyme at 37 °C; the kinetic parameters for $N,N'$-dibenzyl-1,3-diaminopropane were not reported previously. The lower activity of $N,N'$-dibenzyl-1,4-diaminobutane suggested that chemistry is more likely to be rate-limiting with this compound. Consequently, analogues of this compound were selected for further study.

Table 1: Kinetic Parameters of PAO with *para*-Substituted $N,N'$-Dibenzyl-1,4-diaminobutanes as Substrates at pH 8.6, 30 °C

| | kinetic parameter | | |
|---|---|---|---|
| *para*-substituent | $k_{cat}$ ($s^{-1}$) | $k_{cat}/K_m$ ($\mu M^{-1}\ s^{-1}$) | $K_m$ ($\mu$M) |
| $(CH_3)_2N$ | 10.1 ± 0.5 | 0.12 ± 0.02 | 87 ± 15 |
| $CH_3O$ | 4.5 ± 0.1 | 0.24 ± 0.01 | 19 ± 1 |
| $CH_3$ | 3.8 ± 0.3 | 0.35 ± 0.06 | 11 ± 3 |
| H | 0.80 ± 0.02 | 0.054 ± 0.004 | 15 ± 2 |
| Cl | 1.4 ± 0.1 | 0.97 ± 0.30 | 1.4 ± 0.5 |
| Br | 1.8 ± 0.1 | 1.0 ± 0.2 | 1.8 ± 0.4 |
| $CF_3$ | 2.3 ± 0.1 | 0.53 ± 0.10 | 4 ± 2 |

*Steady-State Kinetics.* The steady-state kinetic parameters $k_{cat}$, $k_{cat}/K_m$, and $K_m$ were determined for PAO at pH 8.6 and 30 °C for seven *para*-substituted $N,N'$-dibenzyl-1,4-diaminobutanes as substrates (Table 1). Assays were conducted in air-saturated buffers; therefore, the $k_{cat}$ and $K_m$ values in the table are apparent values, while the $k_{cat}/K_m$ values are independent of the oxygen concentration used.

*$k_{cat}/K_m$–pH Profiles.* The effect of pH on the $k_{cat}/K_m$ value was determined for $N,N'$-dibenzyl-1,4-diaminobutane and the $CH_3O$- and $CF_3$-substituted compounds. These were selected because the $CH_3O$ group is among the most electron-donating of the substituents examined here, while the $CF_3$ group is the most electron-withdrawing. The $k_{cat}/K_m$–pH profiles for all three substrates are bell-shaped curves, and the data fit well to eq 1 (Figure 1A). The p$K_a$ values for all three (Table 2) are within error of each other, with an average value of 8.0 for the p$K_a$ value for a group that must be deprotonated and of 9.9 for the p$K_a$ of a group that must be protonated for activity.

*Steady-State Kinetic Isotope Effects.* Deuterium kinetic isotope effects were determined over the pH range 7.1–10.1 for $N,N'$-dibenzyl-1,4-diaminobutane and the $CH_3O$- and $CF_3$-substituted compounds. The data for all three were fit using eq 2 or 3, which apply for equal isotope effects on $^{D}k_{cat}/K_{DBDB}$ and $^{D}k_{cat}$; alternate equations with different isotope effects on these kinetic parameters did not give improved fits but did give comparable values for the isotope effects. For all three substrates, the isotope effects are less than 2 and are pH-independent (Table 3).

*Flavin Reduction Kinetics.* Stopped-flow experiments were conducted to determine directly the effects that *para*-substituents have on $k_{red}$, the rate constant for flavin reduction at saturating

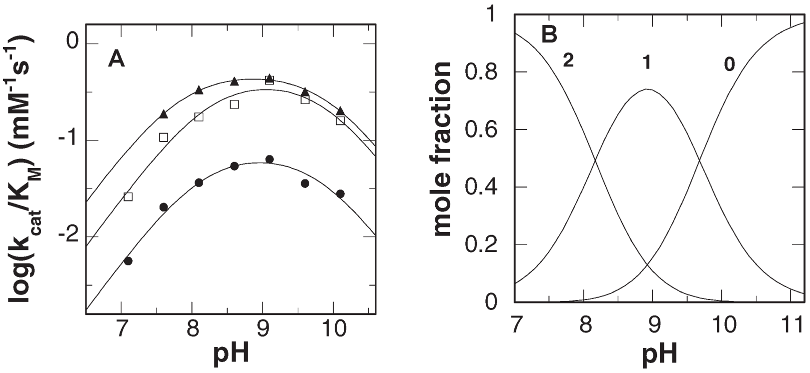

FIGURE 1: (A) $k_{cat}/K_m$−pH profiles for PAO with *N*,*N*′-dibenzyl-1,4-diaminobutane (●), *N*,*N*′-bis(4-$CH_3O$-benzyl)-1,4-diaminobutane (□), and *N*,*N*′-bis(4-$CF_3$-benzyl)-1,4-diaminobutane (▲) as substrates. The average error in the data is 15%. The lines are from fits of the data to eq 1. (B) pH distribution of *N*,*N*′-benzyl-1,4-diaminobutane with zero, one, or two protonated nitrogens.

Table 2: p$K_a$ Values from $k_{cat}/K_m$−pH Profiles for *para*-Substituted *N*,*N*′-Dibenzyl-1,4-diaminobutanes as Substrates for PAO

| X | p$K_1$ | p$K_2$ |
|---|---|---|
| H | 8.1 ± 0.1 | 9.8 ± 0.2 |
| $CH_3O$ | 8.2 ± 0.2 | 9.9 ± 0.2 |
| $CF_3$ | 7.8 ± 0.1 | 9.9 ± 0.1 |

Table 3: Effect of pH on the $^D(k_{cat}/K_m)$ and $^Dk_{cat}$ Values for *para*-Substituted *N*,*N*′-Dibenzyl-1,4-diaminobutanes as Substrates for PAO

| | kinetic isotope effects | | |
|---|---|---|---|
| pH | X = H | X = $CH_3O$ | X = $CF_3$ |
| 7.1 | 1.3 ± 0.1 | 1.7 ± 0.1 | nd[a] |
| 7.6 | 1.7 ± 0.1 | 1.8 ± 0.1 | 1.4 ± 0.1 |
| 8.1 | 1.8 ± 0.1 | 1.7 ± 0.1 | 1.5 ± 0.1 |
| 8.6 | 2.0 ± 0.1 | 1.7 ± 0.1 | 1.6 ± 0.1 |
| 9.1 | 2.1 ± 0.2 | 1.7 ± 0.1 | 1.5 ± 0.1 |
| 9.6 | 2.0 ± 0.2 | 1.6 ± 0.1 | 1.6 ± 0.1 |
| 10.1 | 1.9 ± 0.1 | 1.6 ± 0.1 | 1.6 ± 0.1 |
| average | 1.8 ± 0.3 | 1.7 ± 0.1 | 1.5 ± 0.1 |

[a] nd, not determined.

concentrations of substrate. These results are summarized in Table 4. The reactions were routinely monitored at 458 nm as a function of substrate concentration; with the majority of the substrates, the spectral changes upon mixing enzyme and substrate could be fit to a single exponential decay (Figure 2A). The exception was the $(CH_3)_2N$-substituted compound; in this case the traces were fit better to a double exponential decay (results not shown), where the second rate constant is slower than turnover and therefore not catalytically relevant. These experiments were conducted at both pH 8.6, near the pH optimum, and pH 6.6. In addition, for each substrate a photodiode array detector was used to monitor the spectral changes during the course of the reaction (Figure 2B). Global analyses of the data showed that flavin reduction occurs with no observable intermediates between fully oxidized and fully reduced flavin (Figure 2C). Similar analyses were carried out with the deuterated substrates; the resulting isotope effects on the $k_{red}$ values range from 1.3 to 2.9 and are comparable at pH 8.6 and 6.6 (Table 4). The isotope effects on $k_{red}$ are similar to the isotope effects on $k_{cat}/K_m$ and $k_{cat}$ for those compounds where these were all measured.

Table 4: Rate Constants and Deuterium Kinetic Isotope Effects for Reduction of PAO by *para*-Substituted *N*,*N*′-Dibenzyl-1,4-diaminobutanes

| | pH 6.6 | | pH 8.6 | |
|---|---|---|---|---|
| substituent | $k_{red}$ ($s^{-1}$) | $^Dk_{red}$ | $k_{red}$ ($s^{-1}$) | $^Dk_{red}$ |
| $(CH_3)_2N$ | 2.8 ± 0.3 | 1.4 ± 0.2 | 23.9 ± 0.6 | 1.7 ± 0.1 |
| $CH_3O$ | 1.19 ± 0.01 | 1.8 ± 0.1 | 4.1 ± 0.6 | 1.6 ± 0.2 |
| $CH_3$ | 0.66 ± 0.01 | 1.7 ± 0.1 | 1.84 ± 0.01 | 1.8 ± 0.1 |
| H | 0.21 ± 0.01 | 1.8 ± 0.1 | 0.42 ± 0.02 | 1.5 ± 0.1 |
| Cl | 0.48 ± 0.01 | 2.2 ± 0.1 | 0.80 ± 0.02 | 2.9 ± 0.1 |
| Br | 0.56 ± 0.02 | 1.7 ± 0.1 | 1.04 ± 0.06 | 1.5 ± 0.1 |
| $CF_3$ | 1.05 ± 0.02 | 1.8 ± 0.1 | 1.58 ± 0.06 | 1.3 ± 0.1 |

The effect of pH on the $k_{red}$ value was examined in greater detail with *N*,*N*′-dibenzyl-1,4-diaminobutane as substrate. The $k_{red}$ value has a constant value at low pH and a higher constant value at high pH (Figure 3). Fitting the data to eq 6 yields values for the rate constants at low and high pH of 0.17 ± 0.03 $s^{-1}$ and 1.0 ± 0.20 $s^{-1}$, respectively, with a p$K_a$ value of 8.2 ± 0.3 for the transition.

*Linear Correlation Analysis*. The effect of the substituent at the *para*-position of the aromatic rings on the kinetic parameters was analyzed using single- and multiple-parameter linear correlations. The effect of the substituent on the electronics of the reaction was examined using the parameters $\sigma$, $\sigma^+$, $\sigma^-$, and $\sigma_I$ (*31*). The effect of the hydrophobicity of the substituent was examined using the parameter $\pi$ (*32*). The effect of the size of the substituent was examined using the van der Waals volume, $V_W$ (*33*), and the Taft steric parameter $E_S$ (*34*). (No $E_S$ value is available for the $(CH_3)_2N$ moiety.)

The results of the analyses of the $k_{red}$ value are summarized in Table 5 and Figure 4. The effect of a single parameter was analyzed initially, fitting the data to eq 7. Here, $x$ is the substituent-specific parameter of interest and $C$ is a constant. The best single-parameter correlation is with the van der Waals volume at both pH 8.6 and pH 6.6. However, this correlation is clearly much better at pH 6.6 than at pH 8.6. At both pH values the $\sigma^+$ and the $E_S$ values have the next lowest $\chi^2$ values. Consequently, the data were fit to eq 8, which describes a two-parameter linear correlation using the electronic parameter $\sigma^+$ and $V_W$. (A similar analysis was not done with both $E_S$ and $V_W$ values because $E_S$ values reflect the same phenomenon as $V_W$ values (*35*)). At both pH 8.6 and pH 6.6 the two-parameter analysis with $V_W$ and $\sigma^+$ shows a lower $\chi^2$ value than the single-parameter correlation with just $V_W$. A similar analysis with $\sigma$ and $V_W$ yields a slightly better correlation, although the effect is not

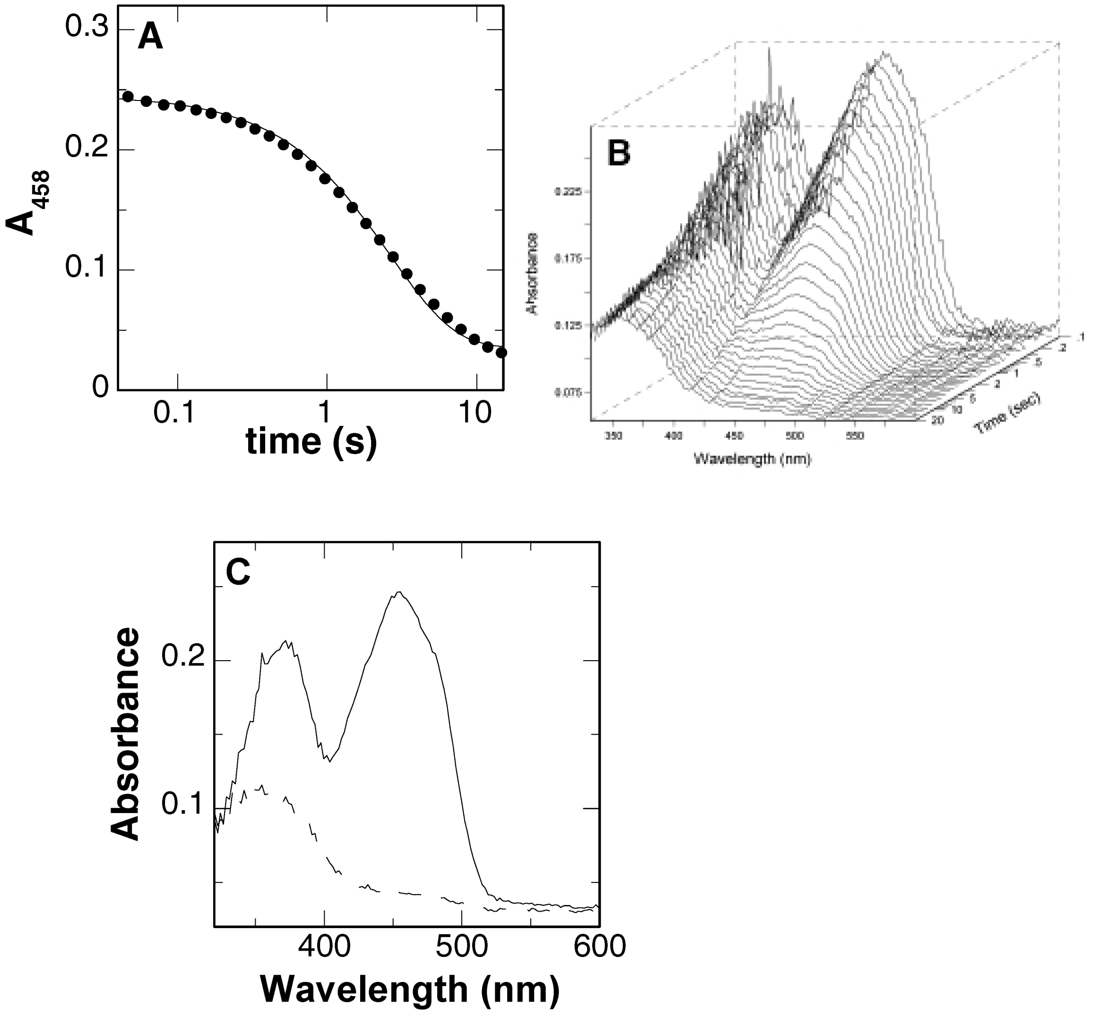

FIGURE 2: Spectral changes during reduction of PAO by $N,N'$-bis(4-$CH_3$-benzyl)-1,4-diaminobutane at pH 6.6, 30 °C: (A) changes at 458 nm (only $^{1}/_{30}$th of the points are shown for clarity); (B) changes in the entire visible absorbance spectrum; (C) initial (—) and final (· · ·) spectra from a global analysis of the data in (B) using a single-step irreversible reaction as the model. The line in (A) is from a fit of the data to eq 4.

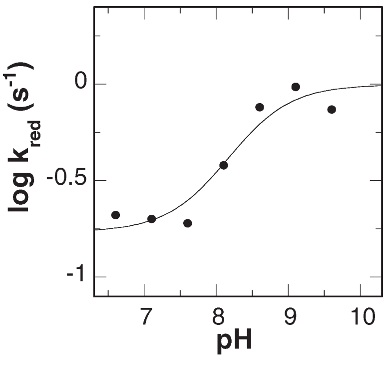

FIGURE 3: pH dependence of $k_{red}$ for PAO oxidation of $N,N'$-dibenzyl-1,4-diaminobutane at 30 °C. The line is from a fit to eq 6.

dramatic. With both $\sigma$ and $\sigma^+$, the $\rho$ value is more negative at pH 8.6 than at pH 6.6, whereas the coefficient for $V_W$ is essentially unaffected by pH.

$$\log k_{red} = Ax + C \qquad (7)$$

$$\log k_{red} = AV_W + \rho\sigma^+ + C \qquad (8)$$

Table 5: Correlation Analyses of log $k_{red}$ for *para*-Substituted $N,N'$-Dibenzyl-1,4-diaminobutanes with Hydrophobic, Steric, and Electronic Parameters

| | pH 6.6 | | pH 8.6 | |
|---|---|---|---|---|
| parameter | coefficient | $\chi^2$ | coefficient | $\chi^2$ |
| $\sigma$ | $-0.45 \pm 0.30$ | 0.53 | $-1.02 \pm 0.36$ | 0.77 |
| $\sigma^+$ | $-0.31 \pm 0.16$ | 0.43 | $-0.64 \pm 0.17$ | 0.53 |
| $\sigma^-$ | $-0.14 \pm 0.50$ | 0.75 | $-0.69 \pm 0.76$ | 1.69 |
| $\sigma_I$ | $0.23 \pm 0.86$ | 0.75 | $-0.37 \pm 1.38$ | 1.94 |
| $\pi$ | $-0.05 \pm 0.40$ | 0.76 | $-0.42 \pm 0.62$ | 1.80 |
| $V_W$ | $0.39 \pm 0.03$ | 0.02 | $0.58 \pm 0.12$ | 0.32 |
| $E_S$ | $-0.20 \pm 0.13$ | 0.23 | $-0.13 \pm 0.20$ | 0.52 |
| $V_W$ | $0.36 \pm 0.02$ | 0.0088 | $0.40 \pm 0.04$ | 0.0156 |
| $\sigma^+$ | $-0.06 \pm 0.03$ | | $-0.37 \pm 0.04$ | |
| $V_W$ | $0.37 \pm 0.02$ | 0.0087 | $0.45 \pm 0.02$ | 0.00702 |
| $\sigma$ | $-0.09 \pm 0.05$ | | $-0.59 \pm 0.04$ | |

The results of similar correlation analyses at pH 8.6 of the effects of the substituents of $N,N'$-dibenzyl-1,4-diaminobutanes on the steady-state kinetic parameters $k_{cat}/K_m$ and $k_{cat}$ are summarized in Table 6. The results of the analyses of the $k_{cat}$ value are very similar to those of the $k_{red}$ value. The best single correlation is with the $V_W$ value. Two-parameter analyses with $V_W$ and $\sigma$ or $V_W$ and $\sigma^+$ are significantly better than the single-parameter correlations. The resulting coefficients are similar to those with $k_{red}$, although in all cases the absolute value of the

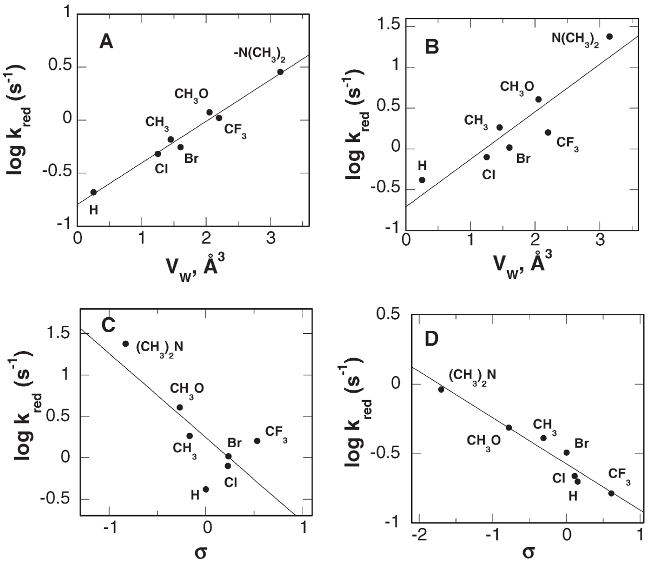

FIGURE 4: Correlation of the $k_{red}$ values for *para*-substituted *N*,*N*′-dibenzyl-1,4-diaminobutanes as substrates for PAO with structural and electronic properties of the substituent: (A) correlation of the $k_{red}$ value at pH 6.6 with the van der Waals volume ($V_W$), (B) correlation of the $k_{red}$ value at pH 8.6 with $V_W$, (C) correlation of the $k_{red}$ value at pH 8.6 with $\sigma$, and (D) correlation of the $k_{red}$ value at pH 8.6 with $\sigma$ after correction of the $k_{red}$ value for the contribution of $V_W$.

Table 6: Correlation Analyses of log $k_{cat}/K_m$ and log $k_{cat}$ with *para*-Substituted *N*,*N*′-Dibenzyl-1,4-diaminobutanes with Hydrophobic, Steric, and Electronic Parameters at pH 8.6

| | $k_{cat}/K_m$ | | $k_{cat}$ | |
|---|---|---|---|---|
| parameter | coefficient | $\chi^2$ | coefficient | $\chi^2$ |
| $\sigma$ | 0.63 ± 0.39 | 0.87 | −0.61 ± 0.24 | 0.36 |
| $\sigma^+$ | 0.31 ± 0.23 | 1 | −0.39 ± 0.13 | 0.28 |
| $\sigma^-$ | 0.76 ± 0.58 | 0.99 | −0.49 ± 0.47 | 0.65 |
| $\sigma_I$ | 2.00 ± 0.71 | 0.52 | −0.32 ± 0.87 | 0.78 |
| $\pi$ | 1.03 ± 0.27 | 0.35 | −0.20 ± 0.40 | 0.76 |
| $V_W$ | 0.06 ± 0.23 | 1.3 | 0.36 ± 0.08 | 0.17 |
| $E_S$ | −0.35 ± 0.18 | 0.71 | −0.11 ± 0.16 | 0.35 |
| $V_W$ | nd | | 0.26 ± 0.08 | 0.072 |
| $\sigma^+$ | nd | | −0.21 ± 0.09 | |
| $V_W$ | 0.23 ± 0.20 | 0.63 | 0.28 ± 0.06 | 0.060 |
| $\sigma$ | 0.86 ± 0.41 | | −0.34 ± 0.13 | |
| $\pi$ | 1.06 ± 0.63 | 0.20 | nd | |
| $\sigma_I$ | 0.73 ± 0.29 | | nd | |
| $E_S$ | −0.13 ± 0.21 | 0.34 | nd | |
| $\sigma_I$ | −0.22 ± 0.85 | | nd | |
| $\pi$ | −0.47 ± 0.54 | 0.28 | nd | |
| $E_S$ | −0.30 ± 0.28 | | nd | |

coefficient is slightly smaller for $k_{cat}$. The correlations for the $k_{cat}/K_m$ value are not as good, in that the low $K_m$ of several of the substrates (Table 1) limited the accuracy with which the $k_{cat}/K_m$ values could be determined. The best linear correlation for $k_{cat}/K_m$ is with the single-parameter $\pi$, giving a coefficient of 1.03 ± 0.27. A two-parameter correlation using both $\pi$ and $\sigma_I$ resulted in an improved fit.

## DISCUSSION

While the physiological substrates for PAO, *N*1-acetylspermine and *N*1-acetylspermidine, contain four and three nitrogen atoms, respectively, the present results clearly show that *N*,*N*′-dibenzyl-1,4-diaminobutanes, with only two nitrogens, are also substrates. This is consistent with earlier reports for partially purified rat PAO that showed that *N*,*N*′-disubstituted diamines can be substrates (*36*). Our previous studies of mouse PAO established that the oxidation of the physiological substrates requires that the nitrogen at the site of CH bond cleavage be neutral and one other nitrogen in the substrate be positively charged (*26*). The $k_{cat}/K_m$−pH profiles for *N*,*N*′-dibenzyl-1,4-diaminobutanes described here are consistent with such a model. The profiles in Figure 1 match well the pH dependence of the fraction of the *N*,*N*′-dibenzyl-1,4-diaminobutane that has only one charged nitrogen (Figure 1B), without a contribution from a protein residue. Thus, as is the case with other flavin amine oxidases (*16*), oxidation of the substrate carbon−nitrogen bond requires that the nitrogen be uncharged. The $k_{red}$−pH profile for *N*,*N*′-dibenzyl-1,4-diaminobutane provides further evidence for such a conclusion. With *N*1-acetylspermine as substrate, the $k_{red}$−pH profile displays a decrease in activity at acidic pH with a p$K_a$ of 7.3 ± 0.1, consistent with the ability of substrate in the incorrectly protonated form to bind to the enzyme but not react (*26*). The $k_{red}$ value for *N*,*N*′-dibenzyl-1,4-diaminobutane similarly decreases at lower pH but reaches a limiting value, in contrast to the results with the much faster physiological substrate. This result raises the possibility that both the protonated and deprotonated forms of *N*,*N*′-dibenzyl-1,4-diaminobutane can react, although the unprotonated form reacts more rapidly. A more likely rationale for the activity at low pH is that the rate constant of ~0.2 $s^{-1}$ is due to loss of the proton from the reacting nitrogen to an amino acid side chain or a water molecule in the active site tunnel. Given the rate constant for this step, this pathway is unlikely to be important for the oxidation of the physiological substrate.

For each of the *N*,*N*′-dibenzyl-1,4-diaminobutanes, the $k_{cat}$ and $k_{red}$ values are comparable, consistent with the reductive half-reaction being substantially rate-limiting for these substrates.[2] This is in contrast to the kinetics for the physiological substrates, where product release is much slower than amine oxidation (*26*). This change in the rate-determining step can be attributed to the much slower oxidation of *N*,*N*′-dibenzyl-1,4-diaminobutanes by PAO, in that the $k_{red}$ values in Table 4 are 2 orders of magnitude smaller than the value for *N*1-acetylspermine (*26*). The kinetic isotope effects provide further evidence for rate-limiting amine oxidation. While extensive steady-state kinetic analyses were only carried out with three of the compounds, the results with these three are quite similar in that the isotope effects on $k_{cat}/K_m$, $k_{cat}$, and $k_{red}$ are essentially identical. The identity of the isotope effects on the $k_{red}$ and $k_{cat}$ values is most consistent with product release being significantly faster than amine oxidation. The pH independence of the isotope effects on the $k_{cat}/K_m$ values establishes that binding steps do not limit amine oxidation (*37*). This leaves amine oxidation as the slow step in turnover.

All of the isotope effects reported here are significantly less than the semiclassical limit of ~7. This raises the possibility that a first-order step prior to carbon−hydrogen bond cleavage partially limits amine oxidation. The agreement of the isotope effects on the $k_{cat}$ and the $k_{cat}/K_m$ values is consistent with the observed isotope effects being the intrinsic ones, but the effects on both kinetic parameters could be suppressed equally by such a step.

---

[2] In several cases the $k_{red}$ values are less than the $k_{cat}$ values. We attribute this to a slight decrease in enzyme activity at the higher enzyme concentrations used in the stopped-flow analysis.

However, there is no evidence for an intermediate in the PAO-catalyzed oxidation of any amine, including those studied here (*20*, *26*). It should be noted that similar small isotope effects have been seen with the flavoprotein amine oxidases LSD1 (*38*) and tryptophan monooxygenase (*21*), both of which are in the MAO structural family, and with D-amino acid oxidase (*39*), which has a different structure. Thus, the combination of steady-state and rapid reaction kinetics is most consistent with CH bond cleavage being the rate-limiting step in the oxidation of *N*,*N*′-dibenzyl-1,4-diaminobutanes by PAO.

Analysis of the effects of the *para* substituents on the kinetics of *N*,*N*′-dibenzyl-1,4-diaminobutanes provides insights into the mechanism of amine oxidation by PAO. The $k_{red}$ value is of most interest, since this is the rate constant for oxidation of the amine. Qualitatively, similar correlations are seen at both pH 8.6 and pH 6.6, in that two-parameter linear correlations with $V_W$ and $\sigma$ show the best fits. The $\sigma$ value is a quantitative measure of the electron-donating or -withdrawing ability of the substituent in the aromatic ring, becoming greater as the substituent becomes less electron-donating (*31*). The quantitative change in a rate constant as a function of the $\sigma$ value provides an indication of the extent of charge development in the transition state for the corresponding reaction. In general, positive $\rho$ values are consistent with development of negative charge, reflecting an increase in rate constants as the substituent becomes more electron-withdrawing. Negative $\rho$ values are consistent with development of positive change, since the rate constants decrease as the substituent becomes more electron-withdrawing. Values close to zero ($\sim -1$ to 1) reflect a lack of charge development.

While the coefficient associated with $V_W$ is pH-independent, going from the pH optimum of 8.6 to pH 6.6 results in an increase in the $\rho$ value from $-0.59$ to $-0.09$. The $\rho$ value at pH 8.6 is likely to be a better description of the degree of charge development in the transition state for carbon−hydrogen bond cleavage, in that the reaction at this pH involves the correctly protonated form of the substrate and therefore no proton loss is required. In contrast, the $\rho$ value at pH 6.6 reflects both the CH bond cleavage step and the requirement that the reactive nitrogen be unprotonated. The p$K_a$ values of *para*-substituted benzylamines correlate well with the $\sigma$ values of the substituents, with the p$K_a$ value of the amine decreasing with an increase in the $\sigma$ value of the substituent, for a $\rho$ value of $-1.1$ (*40*, *41*); this is due to the p$K_a$ value decreasing as the electron-withdrawing ability of the substituent increases. A similar effect is likely for the *para*-substituted *N*,*N*′-dibenzyl-1,4-diaminobutanes studied here (*42*). Since amine oxidation by PAO requires a neutral nitrogen at the site of oxidation, a decrease in the amine p$K_a$ will result in a higher concentration of the reactive species at low pH. Consequently, at low pH a plot of the fraction of the amine with a neutral nitrogen as a function of the $\sigma$ value of the substituent would have a *positive* slope or $\rho$ value. This result would appear to indicate that transition state is electron rich even if the rate constant itself is insensitive to the electron-donating ability of the substituent. This effect of the substituent in the aromatic ring on the amine p$K_a$ value provides a reasonable explanation for the pH dependency of the $\rho$ value for PAO reported here. In the present case, it is the p$K_a$ of the amine when it is bound to the enzyme that is critical. This p$K_a$ is ~8 with *N*,*N*′-dibenzyl-1,4-diaminobutane. The 0.5 increase in the $\rho$ value at pH 6.6 can be attributed to the effect of the substituent in the aromatic ring on the p$K_a$ value of the nitrogen. This is not a problem at pH 8.6, so that the $\rho$ value of $-0.59$ at the higher pH provides a more accurate reflection of the transition state for CH bond cleavage by PAO than the value at pH 6.6. These results also suggest that Hammett analyses of enzyme-catalyzed reactions that do not account for the effects of pH can be misleading.

The $k_{cat}$ value at pH 8.6 exhibits a similar correlation to the $k_{red}$ value, with the best correlation being with the volume and the $\sigma$ value of the *para*-substituent. The absolute values of the coefficients for both parameters are slightly less than those for the $k_{red}$ values. The difference may reflect the lower precision of the steady-state kinetic data or it may reflect attenuation of the effects by a contribution from the product release step. The correlations of the $k_{cat}/K_m$ are not as good, possibly due to the low $K_m$ values of these compounds limiting the accuracy with which $k_{cat}/K_m$ values could be determined. In this case the best correlation is with a combination of $\pi$ and $\sigma_I$. The correlation with $\pi$ can be attributed to the importance of hydrophobic interactions in the binding of substrates to PAO. The active forms of the substrates for PAO, whether the *N*,*N*′-dibenzyl-1,4-diaminobutanes studied here or the physiological substrate *N*1-acetylspermine, are fairly hydrophobic in that they contain only one charged atom. The structure of a mammalian PAO is not available, but structures of maize PAO and the yeast spermine oxidase Fms1 have been determined with bound ligands (*43*, *44*). These structures show that the central carbons and nitrogens of substrates, which the present substrates share with spermine, are mostly involved in hydrophobic interactions with the protein.

The mechanism of flavin amine oxidases has been a source of debate for years, with three possible mechanisms regularly discussed. The single electron transfer mechanism proposed by Silverman (*22*) involves the transient formation of a flavin radical. The polar nucleophilic mechanism proposed by Edmondson (*45*) involves concerted formation of a 4a-alkylated isoalloxazine ring and proton abstraction of the substrate α-hydrogen. Direct transfer of a hydride from the α-C of the substrate to the N5 position of the flavin is the consensus mechanism for the D-amino acid oxidase structural family of flavin amine oxidases (*16*, *46*); its applicability to the MAO structural family is supported by kinetic isotope effects and the failure to detect intermediates in the reactions of these enzymes (*17*−*20*, *38*, *45*). The $\rho$ value of $-0.59$ for PAO at pH 8.6 reported here is most consistent with a direct hydride transfer reaction in which there is little charge development in the transition state for carbon−hydrogen bond cleavage. This value would also be consistent with the expectations for abstraction of a hydrogen atom from the carbon of the substrate (*47*), but such a reaction is unlikely for a flavin given the energetics of such a reaction. Indeed, the various radical mechanisms proposed for flavin-catalyzed amine oxidation involve initial formation of an aminium radical rather than a carbon-based radical (*22*, *48*). The lack of detectable intermediates in the reductive half-reaction of PAO is also consistent with direct hydride transfer from the amine to the flavin.

Hammett analyses have been carried out with other flavin amine oxidases. When a series of *para*-substituted phenylglycines were used as substrates for a yeast D-amino acid oxidase, the $k_{red}$ values correlated well with a combination of the $V_W$ and $\sigma^+$ values of the substituents, yielding a $\rho$ value of $-0.73$ (*49*), in line with the expectations for a hydride transfer mechanism for this structural family of amine oxidase, and very similar to the results reported here. Several analyses of MAO have been described with somewhat contradictory results. With MAO A (*45*), there is a positive correlation between the $k_{red}$ values for a series of

12 ring-substituted benzylamines and the electronic parameter $\sigma$ with a $\rho$ value of 2, while the $k_{red}$ values for four additional compounds give a $\rho$ value of 0.5.[3] The $\rho$ value of 2 has been interpreted as evidence for removal of the substrate α-hydrogen as a proton (*23*). In contrast, the $k_{red}$ value for oxidation of substituted phenethylamines by MAO A shows no correlation with any $\sigma$ parameter; instead, the value correlates best with the size of the substituent, measured as either $V_W$ or $E_S$, with larger substrates reacting more slowly (*50*). As noted at the time, the extra methylene in phenethylamines versus benzylamines is expected to attenuate the electronic effects of substituents. However, this effect typically yields only a 2−3-fold reduction in the $\rho$ value (*51*). The lack of any correlation of the $k_{red}$ values for oxidation of phenylethylamines by MAO A with $\sigma$ values was attributed to dominant steric effects masking the electronic effects (*50*). In the case of MAO B, the $k_{red}$ values for substituted benzylamines correlate best with a combination of $\pi$ and $V_W$ (*52*), in good agreement with the results for MAO A and phenethylamines. The present results with PAO are in line with the earlier results for D-amino acid oxidase and MAO B and with the results for MAO A with phenethylamines, but are clearly different from the results with MAO A and benzylamines. This discrepancy can be rationalized in a variety of ways. Oxidation of benzylamines by MAO A could occur by a different mechanism from amine oxidation by MAO B, PAO, and other flavin amine oxidases. This seems unlikely given the structural similarities of these enzymes (*12*, *23*). Alternatively, the electronic effects of the substituents in the oxidation of benzylamines by MAO B could be suppressed due to the restrictive active site of that enzyme preventing the required orbital alignment of the benzyl carbon with the aromatic ring (*23*). Such an explanation could also be invoked for the results with PAO described here. In that case, the reactions of MAO A and B, and presumably PAO, would involve a cationic transition state, in line with the predictions for a mechanism involving nucleophilic attack of the amine on the flavin. Such an explanation would require different mechanisms of amine oxidation by the D-amino acid oxidase and MAO structural families. However, deuterium and $^{15}N$ kinetic isotope effects for D-amino acid oxidase are indistinguishable from those for an L-amino acid oxidase (*18*, *53*), suggesting that they have similar mechanisms. L-Amino acid oxidases are in the MAO structural family, and their structures are more consistent with hydride transfer than nucleophilic mechanism (*11*, *54*). Moreover, *ab initio* calculations show that the $^{15}N$ isotope effects for both enzymes are inconsistent with nucleophilic mechanisms (*19*). Thus, the large $\rho$ value for oxidation of benzylamines by MAO A would require that MAO A and B have a mechanism different from structurally similar flavin amine oxidases (*23*). Another possibility is that the $\rho$ value of 2 with MAO A reflects at least in part the effects of substituents on the p$K_a$ values of benzylamines, since the measurements were carried out below the p$K_a$ seen in the $k_{red}$−pH profile for benzylamine (*55*).

The studies described here provide further insights into the mechanism of PAO and the entire MAO structural family. The ability to oxidize *N*,*N*′-dibenzyl-1,4-diamines establishes that two nitrogens in a substrate are sufficient for oxidation by PAO. The pH dependence of the $k_{cat}/K_m$ and $k_{red}$ values confirms the need for a neutral nitrogen at the site of oxidation. The effects of substituents in the aromatic ring on the kinetics of oxidation are most consistent with a direct hydride transfer from the neutral CN bond of the substrate.

---

[3] When the $k_{red}$ values for MAO A for all of the substituted benzylamines are combined in a single analysis, the $\rho$ value is 0.93 ± 0.25, closer to the expectations for hydride transfer.

## REFERENCES

1. Casero, R. A., Jr., and Marton, L. J. (2007) Targeting polyamine metabolism and function in cancer and other hyperproliferative diseases. *Nat. Rev. Drug Discovery 6*, 373–390.
2. Marton, L. J., and Pegg, A. E. (1995) Polyamines as targets for therapeutic intervention. *Annu. Rev. Pharmacol. Toxicol. 35*, 55–91.
3. Wang, Y., and Casero, R. A., Jr. (2006) Mammalian polyamine catabolism: a therapeutic target, a pathological problem, or both? *J. Biochem.* (*Tokyo*) *139*, 17–25.
4. Pegg, A. E. (2008) Spermidine/spermine-N1-acetyltransferase: a key metabolic regulator. *Am. J. Physiol. Endocrinol. Metab. 294*, E995–E1010.
5. Wu, T., Yankovskaya, V., and McIntire, W. S. (2003) Cloning, sequencing, and heterologous expression of the murine peroxisomal flavoprotein, N1-acetylated polyamine oxidase. *J. Biol. Chem. 278*, 20514–20525.
6. Seiler, N., Peter, M., Yu, K. F. T., and Alan, A. B. (1995) Polyamine oxidase, properties and functions. *Prog. Brain Res. 106*, 333–344.
7. Wang, Y., Devereux, W., Woster, P. M., Stewart, T. M., Hacker, A., and Casero, R. A., Jr. (2001) Cloning and characterization of a human polyamine oxidase that is inducible by polyamine analogue exposure. *Cancer Res. 61*, 5370–5373.
8. Vujcic, S., Diegelman, P., Bacchi, C. J., Kramer, D. L., and Porter, C. W. (2002) Identification and characterization of a novel flavin-containing spermine oxidase of mammalian cell origin. *Biochem. J. 367*, 665–675.
9. Binda, C., Newton-Vinson, P., Hubalek, F., Edmondson, D. E., and Mattevi, A. (2002) Structure of human monoamine oxidase B, a drug target for the treatment of neurological disorders. *Nat. Struct. Biol. 9*, 22–26.
10. Chen, Y., Yang, Y., Wang, F., Wan, K., Yamane, K., Zhang, Y., and Lei, M. (2006) Crystal structure of human histone lysine-specific demethylase 1 (LSD1). *Proc. Natl. Acad. Sci. U.S.A. 103*, 13956–13961.
11. Pawelek, P. D., Cheah, J., Coulombe, R., Macheroux, P., Ghisla, S., and Vrielink, A. (2000) The structure of L-amino acid oxidase reveals the substrate trajectory into an enantiomerically conserved active site. *EMBO J. 19*, 4204–4215.
12. Binda, C., Mattevi, A., and Edmondson, D. E. (2002) Structure-function relationships in flavoenzyme dependent amine oxidations. A comparison of polyamine oxidase and monoamine oxidase. *J. Biol. Chem. 277*, 23973–23976.
13. Sebela, M., Radová, A., Angelini, R., Tavladoraki, P., Frébort, I., and Pec, P. (2001) FAD-containing polyamine oxidases: a timely challenge for researchers in biochemistry and physiology of plants. *Plant Sci. 160*, 197–207.
14. Landry, J., and Sternglanz, R. (2003) Yeast Fms1 is a FAD-utilizing polyamine oxidase. *Biochem. Biophys. Res. Commun. 303*, 771–776.
15. Bright, H. J., and Porter, D. J. T. (1975) Flavoprotein oxidases, in The Enzymes (Boyer, P., Ed.) 3rd ed., Vol. XII, pp 421−505, Academic Press, New York.
16. Fitzpatrick, P. F. (2010) Oxidation of amines by flavoproteins, Arch. Biochem. Biophys. (in press).
17. Miller, J. R., Edmondson, D. E., and Grissom, C. B. (1995) Mechanistic probes of monoamine oxidase B catalysis: rapid-scan stopped flow and magnetic field independence of the reductive half-reaction. *J. Am. Chem. Soc. 117*, 7830–7831.
18. Ralph, E. C., Anderson, M. A., Cleland, W. W., and Fitzpatrick, P. F. (2006) Mechanistic studies of the flavoenzyme tryptophan 2-monooxygenase: deuterium and $^{15}N$ kinetic isotope effects on alanine oxidation by an L-amino acid oxidase. *Biochemistry 45*, 15844–15852.
19. Ralph, E. C., Hirschi, J. S., Anderson, M. A., Cleland, W. W., Singleton, D. A., and Fitzpatrick, P. F. (2007) Insights into the mechanism of flavoprotein-catalyzed amine oxidation from nitrogen isotope effects on the reaction of N-methyltryptophan oxidase. *Biochemistry 46*, 7655–7664.
20. Royo, M., and Fitzpatrick, P. F. (2005) Mechanistic studies of mouse polyamine oxidase with N1,N12-bisethylspermine as a substrate. *Biochemistry 44*, 7079–7084.
21. Emanuele, J. J., Jr., and Fitzpatrick, P. F. (1995) Mechanistic studies of the flavoprotein tryptophan 2-monooxygenase. 2. pH and kinetic isotope effects. *Biochemistry 34*, 3716–3723.

22. Silverman, R. B. (1995) Radical ideas about monoamine oxidase. *Acc. Chem. Res. 28*, 335–342.
23. Edmondson, D. E., Binda, C., and Mattevi, A. (2007) Structural insights into the mechanism of amine oxidation by monoamine oxidases A and B. *Arch. Biochem. Biophys. 464*, 269–276.
24. Paik, C. Y., Metaferia, B., Tang, S., Bane, S., Ravindra, R., Shanker, N., Alcaraz, A. A., Johnson, S. A., Schaefer, J., O'Connor, R. D., Cegelski, L., Snyder, J. P., and Kingston, D. G. I. (2007) Rotational-echo double-resonance NMR distance measurements for the tubulin-bound paclitaxel conformation. *J. Am. Chem. Soc. 129*, 361–370.
25. Burns, M. R., LaTurner, S., Ziemer, J., McVean, M., Devens, B., Carlson, C. L., Graminski, G. F., Vanderwerf, S. M., Weeks, R. S., and Carreon, J. (2002) Induction of apoptosis by aryl-substituted diamines: role of aromatic group substituents and distance between nitrogens. *Bioorg. Med. Chem. Lett. 12*, 1263–1267.
26. Henderson Pozzi, M., Gawandi, V., and Fitzpatrick, P. F. (2009) pH dependence of a mammalian polyamine oxidase: insights into substrate specificity and the role of lysine 315. *Biochemistry 48*, 1508–1516.
27. Cleland, W. W. (1979) Statistical analysis of enzyme kinetic data. *Methods Enzymol. 63*, 103–138.
28. Schimerlik, M. I., Grimshaw, C. E., and Cleland, W. W. (1977) Determination of the rate-limiting steps for malic enzyme by the use of isotope effects and other kinetic studies. *Biochemistry 16*, 571–576.
29. Fitzpatrick, P. F., Valley, M. P., Bozinovski, D. M., Shaw, P. G., Héroux, A., and Orville, A. M. (2007) Mechanistic and structural analyses of the roles of Arg409 and Asp402 in the reaction of the flavoprotein nitroalkane oxidase. *Biochemistry 46*, 13800–13808.
30. Bolkenius, F. N., and Seiler, N. (1981) Acetylderivatives as intermediates in polyamine catabolism. *Int. J. Biochem. 13*, 287–292.
31. Hansch, C., Leo, A., and Taft, R. W. (1991) A survey of Hammett substituent constants and resonance and field parameters. *Chem. Rev. 91*, 165–195.
32. Fujita, T., Iwasa, J., and Hansch, C. (1964) A new substituent constant, $\pi$, derived from partition coefficients. *J. Am. Chem. Soc. 86*, 5175–5180.
33. Bondi, A. (1964) van der Waals volumes and radii. *J. Phys. Chem. 68*, 441–451.
34. Hansch, C., Leo, A., and Hoekman, D. (1995) Exploring QSAR, Volume 2: Hydrophobic, Electronic, and Steric Constants , American Chemical Society, Washington, DC.
35. Charton, M. (1969) Nature of the ortho effect. II. Composition of the Taft steric parameters. *J. Am. Chem. Soc. 91*, 615–618.
36. Bolkenius, F. N., and Seiler, N. (1989) New substrates of polyamine oxidase dealkylation of N-alkyl-α,*o*-diamines. *Biol. Chem. Hoppe-Seyler 370*, 525–531.
37. Cook, P. F., and Cleland, W. W. (1981) pH variation of isotope effects in enzyme-catalyzed reactions. 1. Isotope- and pH-dependent steps the same. *Biochemistry 20*, 1797–1805.
38. Gaweska, H., Henderson Pozzi, M., Schmidt, D. M. Z., McCafferty, D. G., and Fitzpatrick, P. F. (2009) Use of pH and kinetic isotope effects to establish chemistry as rate-limiting in oxidation of a peptide substrate by LSD1. *Biochemistry 48*, 5440–5445.
39. Denu, J. M., and Fitzpatrick, P. F. (1992) pH and kinetic isotope effects on the reductive half-reaction of D-amino acid oxidase. *Biochemistry 31*, 8207–8215.
40. Blackwell, L. F., Fischer, A., Miller, I. J., Topsom, R. D., and Vaughan, J. (1964) Dissociation of benzylammonium ions. *J. Chem. Soc.,* 3588–3591.
41. Peters, F. B., and Johnson, H. W., Jr. (1975) Ionization constants of substituted 2-aminoacetanilides and benzylamines. Transmission of electronic effects through amide links. *J. Org. Chem. 40*, 1517–1519.
42. Clark, J., and Perrin, D. D. (1964) Prediction of the strengths of organic bases. *Q. Rev. Chem. Soc. 18*, 295–320.
43. Binda, C., Angelini, R., Federico, R., Ascenzi, P., and Mattevi, A. (2001) Structural bases for inhibitor binding and catalysis in polyamine oxidase. *Biochemistry 40*, 2766–2776.
44. Huang, Q., Liu, Q., and Hao, Q. (2005) Crystal structures of Fms1 and its complex with spermine reveal substrate specificity. *J. Mol. Biol. 348*, 951–959.
45. Miller, J. R., and Edmondson, D. E. (1999) Structure-activity relationships in the oxidation of para-substituted benzylamine analogues by recombinant human liver monoamine oxidase A. *Biochemistry 38*, 13670–13683.
46. Fitzpatrick, P. F. (2004) Carbanion versus hydride transfer mechanisms in flavoprotein-catalyzed dehydrogenations. *Bioorg. Chem. 32*, 125–139.
47. Fitzpatrick, P. F., Flory, D. R., Jr., and Villafranca, J. J. (1985) 3-Phenylpropenes as mechanism-based inhibitors of dopamine $\beta$-hydroxylase: evidence for a radical mechanism. *Biochemistry 24*, 2108–2114.
48. Scrutton, N. S. (2004) Chemical aspects of amine oxidation by flavoprotein enzymes. *Nat. Prod. Rep. 21*, 722–730.
49. Pollegioni, L., Blodig, W., and Ghisla, S. (1997) On the mechanism of D-amino acid oxidase. Structure/linear free energy correlations and deuterium kinetic isotope effects using substituted phenylgylcines. *J. Biol. Chem. 272*, 4924–4934.
50. Nandigama, R. K., and Edmondson, D. E. (2000) Structure-activity relations in the oxidation of phenethylamine analogues by recombinant human liver monoamine oxidase A. *Biochemistry 39*, 15258–15265.
51. Taft, R. W., and Lewis, I. C. (1969) Evaluation of resonance effects on reactivity by application of the linear inductive energy relationship. V. Concerning a $\sigma_R$ scale of resonance effects. *J. Am. Chem. Soc. 81*, 5343–5352.
52. Walker, M. C., and Edmondson, D. E. (1994) Structure-activity relationships in the oxidation of benzylamine analogues by bovine liver mitochondrial monoamine oxidase B. *Biochemistry 33*, 7088–7098.
53. Kurtz, K. A., Rishavy, M. A., Cleland, W. W., and Fitzpatrick, P. F. (2000) Nitrogen isotope effects as probes of the mechanism of D-amino acid oxidase. *J. Am. Chem. Soc. 122*, 12896–12897.
54. Faust, A., Niefind, K., Hummel, W., and Schomburg, D. (2007) The structure of a bacterial L-amino acid oxidase from *Rhodococcus opacus* gives new evidence for the hydride mechanism for dehydrogenation. *J. Mol. Biol. 367*, 234–248.
55. Dunn, R. V., Marshall, K. R., Munro, A. W., and Scrutton, N. S. (2008) The pH dependence of kinetic isotope effects in monoamine oxidase A indicates stabilization of the neutral amine in the enzyme-substrate complex. *FEBS J. 275*, 3850–3858.